On the potential of using photoacoustic spectroscopy for monitoring red blood cell aggregation

Eno Hysi[a], Ratan K. Saha[a,b], and Michael C. Kolios[a*]
[a]Department of Physics, Ryerson University, Toronto, Canada;
[b]Applied Materials Science Division, Saha Institute of Nuclear Physics, Kolkata, India

ABSTRACT

In this paper we examine the potential of using photoacoustic (PA) spectroscopy for the monitoring of red blood cell (RBC) aggregation phenomena. The process of RBC aggregation has been shown to occur during periods of increased plasma fibrinogen concentration and periods of decreased blood flow (leading to diminished shear forces on the aggregates). Current techniques used to monitor RBC aggregation are invasive and do not provide an accurate assessment of the aggregation process *in-vivo*. We present a theoretical model for investigating the potential of PA spectroscopy for detecting and characterizing the aggregation phenomenon. We show that the signal strength increases with RBC aggregation. Experimental confirmation of the theoretical predictions is provided. Our theoretical and experimental results suggest the PA spectroscopy is capable of monitoring RBC aggregation and providing important information about changes that occur during the aggregation process as it pertains to the dynamics of aggregate formation.

Keywords: Photoacoustics, red blood cell aggregation, spectroscopy, Monte Carlo simulations

1. INTRODUCTION

1.1 The phenomenon of red blood cell aggregation

Human red blood cells (RBCs) tend to align themselves and form structures that resemble a stack of coins. Such structures are known as rouleaux and the process is termed RBC aggregation. Figure 1 shows a representative sample of bovine and porcine RBCs suspended in autologous plasma[1]. Bovine blood does not form rouleaux while porcine blood can form extensive network of rouleaux. During aggregation, there is significant branching of individual rouleau while the number of RBC per rouleau varies (figure 1 right panel). It is important to note that while bovine and porcine RBCs have differing intrinsic tendencies to form aggregates, the morphological properties of these images closely resemble what is observed in non-aggregating and aggregating conditions of human blood.

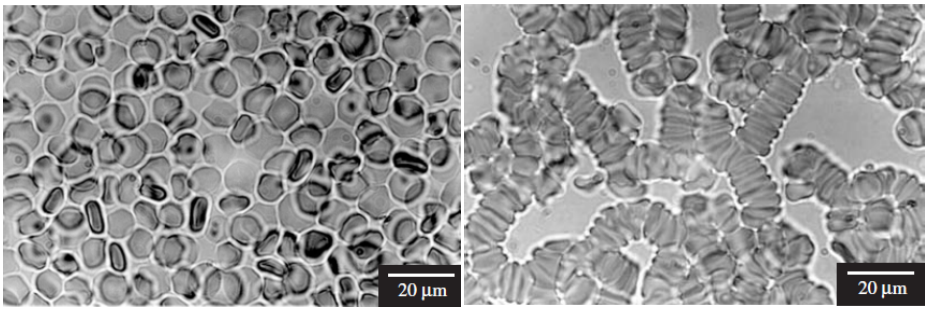

Figure 1. Bovine (left panel) and porcine (right panel) RBCs suspended in autologous plasma. Figure adapted from reference[1].

* mkolios@ryerson.ca

Dynamics and Fluctuations in Biomedical Photonics IX, edited by Valery V. Tuchin, Donald D. Duncan, Kirill V. Larin, Martin J. Leahy, Ruikang K. Wang, Proc. of SPIE Vol. 8222, 82220Q · © 2012 SPIE · CCC code: 1605-7422/12/$18 · doi: 10.1117/12.928257

Downloaded from SPIE Digital Library on 19 Feb 2012 to 141.117.54.100. Terms of Use: http://spiedl.org/terms

The aggregation of RBCs is regulated by the balance between the forces promoting and those preventing aggregation from occurring. However, the mechanism of RBC aggregation has not been fully understood. There is general agreement that aggregation is associated with the presence of plasma macromolecules such as fibrinogen[2]. It has also been observed to occur in aqueous suspensions of polymers such as dextran or derivatives of poloxamers. RBC aggregation does not take place in salt solutions such as phosphate-buffered saline (PBS). These observations have prompted two mutually exclusive models on the mechanism of RBC aggregation. The first model, the bridging model, proposes that the aggregation occurs due to the cross-linking of plasma macromolecules (i.e. fibrinogen) in the binding site of adjacent cells[3]. The second model, the depletion model, proposes the opposite: RBCs aggregate due to the osmotic gradient caused by the reduction in the localization of polymers near the cell surface compared to the surrounding medium[4]. This leads to the depletion of the polymer near the cell surface thus bringing the cells in closer proximity. Studies in literature support both models but conclusive evidence is lacking[5].

RBC aggregation is also affected by the shear forces and the membrane strain, factors that both prevent rouleaux formation[5]. Shear forces can arise due to blood velocity gradients created as blood flows through vessels. Rouleau formation is prevented when the magnitude of the shear forces is greater than the forces that keep the RBC aggregates together. No aggregation is observed in normal blood aggregates for shear rates higher than 20-40 s^{-1}, while pathologic blood requires higher shear rates for disaggregation. Higher blood viscosity has been observed in the presence of RBC aggregation. Furthermore, aggregation requires the RBCs to deform enough in order to accommodate stacking of the cells. The membrane strain opposes this deformation and decreases RBC aggregation. The effect of shear rate and membrane strain on the viscosity of RBC suspensions is shown in figure 2. When comparing non-aggregating RBCs (suspended in saline) and rigid RBCs (with increased membrane strain due to fixing with aldehydes), the viscosity is more than 4 times lower in autogolous plasma capable of forming aggregates for shear rates < 20 s^{-1} compared to blood.

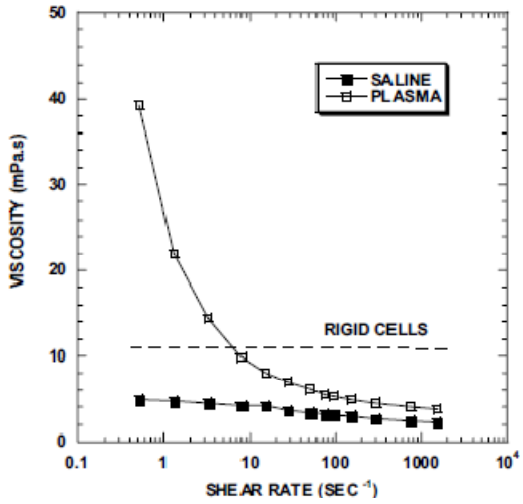

Figure 2. Representative viscosity versus shear rate data for three types of RBC suspensions at 40% hematocrit. The suspensions are human RBCs in saline (black squares), autologous plasma (white squares) and aldehyde solution (dashed line). Figure was adapted from reference[6].

Although there have been several studies investigating the alterations of RBC aggregation in the human circulation, it is difficult to define the "normal" range of RBC aggregation. This is due to the physical basis of these measurements (i.e. how aggregation is assessed) and the nature of the measured aggregation parameters as determined by the various approaches and instruments which requires careful interpretation of these parameters. There is however general agreement that enhanced aggregation is observed and associated with a variety of pathophysiological processes. The reported conditions where enhanced RBC aggregation has been observed or measured are: inflammatory conditions[7], infections[8] (i.e. sepsis and septic shocks), cardiovascular conditions[9] (i.e. hypertension, atherosclerosis, myocardial ischemia and infarction, cerebral ishchemia and stroke) and metabolic conditions[10] (i.e. diabetes and obesity). In addition to the physiological abnormalities where aggregation is observed, under normal conditions, variations in RBC aggregation have been reported due to subject gender, age, pregnancy, physical activity and extreme environmental conditions[5].

Downloaded from SPIE Digital Library on 19 Feb 2012 to 141.117.54.100. Terms of Use: http://spiedl.org/terms

1.2 Measurements of RBC aggregation

While prominent changes in RBC aggregation can be observed in a variety of diseases, there is no widely accepted method for the detection and characterization of RBC aggregation. Depending on the parameter to be investigated (i.e. extent of aggregation, the time course of aggregation or the magnitude of forces holding aggregates together) several techniques can be used.

The oldest and one of the most widely used in clinical laboratories is the erythrocytes sedimentation rate[11]. This technique measures the rate at which RBCs sediment from the plasma of whole blood. The method is however time consuming and has strong hematocrit dependence. Therefore, the technique cannot distinguish between aggregation and other hematocrit depended disorders such as anemia. The microscopic index of aggregation (MAI) is also used as a method for assessing the average number of aggregates in a blood sample. The MAI is obtained by dividing the non-aggregated RBC count by the number of the overall cellular units (aggregated and non-aggregated) in the sample being analyzed but it does not provide any information about the aggregation time course[12].

Optical techniques are used to measure changes in transmitted or reflected light intensity from a RBC sample as a function of time and shearing condition. The samples are typically exposed to high shear rates (500 s^{-1}) for ~ 10 s during which the RBCs disaggregate thus mostly reflecting the transmitted light. Abruptly stopping the shearing forms aggregates thus increasing transmitted light intensity. These curves known as syllectograms yield a series of parameters and indexes of aggregation reflecting the time and extent of the aggregation process[13]. Their interpretation however depends on the measurement apparatus since there is no aggregation standard making it hard to use these parameters for making *in-vivo* assessments of RBC aggregation levels.

Ultrasound (US) backscattering methods have also been used for characterizing suspensions of blood[14]. As the size of the RBCs is much smaller than the ultrasound wavelengths at clinical frequencies, the RBCs can be considered Rayleigh scatters. Rayleigh scattering theory predicts that the scattering power of the RBCs increases with the forth power of the ultrasound frequency and the square of the scatterer volume. This relationship could change when the aggregate size increases. The US backscattering was thus shown to be depended on the shear rate of the flowing tubes and the concentration of fibrinogen and dextrans in the suspending medium[15]. Even though the monitoring of US backscattering has been used as a method to estimate aggregate size *in-vitro*, US-based methods are yet not well established for *in-vivo* applications. This is due to the fact that during US exams one cannot control the shearing conditions thus making it difficult to compare the parameters obtained from such techniques with the control conditions during the same exam. In addition, the ultrasound backscatter does not monotonically increase with increasing hematocrit; the backscatter as a function of hematocrit peaks at a certain hematocrit level (which depends on the ultrasound frequency), monotonically decreasing thereafter. This well-known phenomenon is due to the fact that the ultrasound waves scattered from RBCs may interfere constructively or destructively depending on the relationship between the spatial distribution of the RBCs and the ultrasound wavelength, in a manner somewhat similar to Bragg scattering[16].

1.3 Photoacoustics and its potential to characterize blood

Photoacoustics (PA) refers to the production of acoustic waves due to the interaction of incident light with the material it is absorbed in. In PA imaging acoustic waves are produced from the transient thermoelastic expansion due to the absorption of incident optical energy[17]. Unlike high-resolution pure optical methods, PA imaging does not depend on the variation of the reflected or transmitted light but rather on the detection of the generated sound waves. This is an inherent advantage of PA over pure optical imaging since sound waves scatter 2-3 orders of magnitude less than optical waves in tissue, allowing deeper imaging in strongly scattering media[18]. As a result, PA combines the high spatial resolution provided by detecting the induced ultrasonic waves with the contrast provided by exploiting the inherent absorption of tissues using optical wavelengths.

PA imaging has been used to provide information about physiology or exogenously administered optical absorbers through high contrast and resolution images[19]. Most PA techniques used in biomedicine make advantage of the difference in the optical absorption spectra of oxygenated and deoxygenated blood, an advantage over the structural only information provided by US imaging. The optical absorption of blood is entirely due to hemoglobin, the most abundant protein inside RBCs whose primary role is to facilitate the release/capture cycle of oxygen in the lungs and tissue. PA is capable of differentiating between the different states of hemoglobin oxygenation using multiple wavelengths to probe

Downloaded from SPIE Digital Library on 19 Feb 2012 to 141.117.54.100. Terms of Use: http://spiedl.org/terms

the peak absorption of blood for each oxygenation state. For instance, the two wavelength approach has been used for imaging cerebral hemoglobin concentration and oxygenation non-invasively in addition to forming high resolution oxygenation maps of small animal brains[20]. In addition to oxygenation dependent studies, PA has been explored as a tool for molecular imaging applications[21]. Gold nanoparticles with high optical absorption can be targeted to specific cancer biomarkers and thus can be used for the non-invasive detection and monitoring of cancer at the molecular level. Such targeting of nanoparticles helps in early detection of cancer due to the large difference in optical absorption between the particles and tissues. This enhances the contrast of PA images and in conjunction with US images can provide dual information about the structure and physiology of the tumors being targeted. Moreover, our group has explored the potential of PA for the detection of normal and abnormal vasculature[22], monitoring thermal therapy[23], estimation of optical and thermomechanical properties of tissue[24] and optical vaporization of nano-droplets (optical droplet vaporization - OVD) for cancer therapy and imaging[25].

Almost all PA techniques used described thus far make use of the time-domain ultrasonic signals generated from the irradiated volume of interest. These signals are typically broadband. It is well established that the frequency-domain response from optical absorbers heavily depends on the size of the absorber[26]. Therefore, the transducer used for recording the PA signals will have a significant impact in the ability of the PA system to maintain the high resolution for imaging biological systems. Analysis of frequency content of the ultrasound radio-frequency (RF) signals is extensively used for ultrasound tissue characterization techniques[27] and therapy response monitoring[28] as the size of the scattering structure modulates the frequency of the scattered ultrasound, allowing the characterization of collections of non-resolvable scattering structures. In a similar manner, we postulate that based on the known frequency dependence of the PA ultrasound signals as a function of absorber size, analysis of the frequency dependence of the detected PA RF transients will provide information about the absorbing structure size. By using the spectral information contained in the signals, one can take into account the system response by subtracting the signal spectrum from the spectrum of the transducer response, as is done in classical ultrasonic tissue characterization techniques. Performing linear regression on the normalized spectrum yields a set of parameters (such as the slope and midband fit) that can be related to structural tissue properties such as scatterer size, acoustic impedance and concentration (in ultrasound tissue characterization). In the case of PA RF analysis, the absorber size, optical properties and concentration can also be related to the parameters that are obtained from the spectroscopic analysis of PA signals. We thus propose using spectroscopic analysis on the PA RF ultrasonic signals in order to detect and characterize the aggregation of RBCs.

2. METHODOLOGY

2.1 Theoretical modeling of RBC aggregation

The theoretical model and simulations developed for studying the PA response from non-aggregated and aggregated RBCs were described in detail at recent publications from our group[29,30]. In brief, a simulation protocol based on Monte Carlo methods was developed to compute the frequency-domain PA pressure from a collection of spheres representing individual RBCs. The cells were then packed using a hexagonal packing scheme into compact spherical aggregates representing aggregating RBCs of varying sizes. The non band-limited pressure field generated by spherical sources uniformly irradiated by a laser with a delta function heating pulse was computed by extending the theoretical model used by Diebold[26]. In a more recent study, the effect of incorporating a finite transducer bandwidth for the detection of PA signals from such collections was examined[31].

For this paper, analysis was performed on the theoretical power spectra for non-aggregated and aggregated RBCs. More specifically, the theoretical PA signals obtained from the original theoretical model generated in the first publication on this work were filtered by the Gaussian response of a 5 MHz transducer in order to obtain the band-limited signals that are measured in practice during PA experiments. These band-limited spectra were then normalized by the response of the transducer used to filter them and spectroscopic analysis was performed on the normalized spectra by extracting parameters (midband fit, spectral slope), which are related to tissue properties such as the size and concentration of the absorbers that are RBCs.

2.2 Experimental monitoring of RBC aggregation with PA

Several experiments on using PA for the detection and characterization of RBC aggregation were reported at recent publications from our group[31–33]. For this paper, porcine blood was used as the aggregation model. The blood was

Downloaded from SPIE Digital Library on 19 Feb 2012 to 141.117.54.100. Terms of Use: http://spiedl.org/terms

extracted from pigs onto EDTA vacutaners (Becton, Dickinson and Company, Franklin Lakes, NJ). The RBCs were extracted upon centrifugation of the whole blood and removal of the plasma and white blood cells. The washed cells were re-suspended in phosphate buffered saline at various hematocrit levels (10, 20 and 40%). Aggregation was induced with Dextran-70 at concentrations of 1, 3 and 8% (wt/vol) at each hematocrit level as the non-aggregated RBCs. PA measurements were performed using the Imagio Small Animal PA imaging device (Seno Medical Instruments Inc., San Antonio, TX). The device contains a 1064 nm Nd:YAG laser emitting 6 ns pulses with 10 Hz pulse repetition rate with a fluence of 2.5 mW/cm^2. It contains a 4 channel annular array with central frequency of 5 MHz and -6 dB bandwidth of 2-8 MHz. Samples of RBCs were placed inside a Tygon tube (Norton Performance Plastic, Akron, OH) and the laser emitted 4 pulses at each location while raster scanning the entire tube. The spectroscopic analysis was performed by dividing the PA RF power spectrum for each measurement by the PA RF power spectrum obtained from a 200 nm thick gold film which provided the frequency response of the transducer. The PA signal amplitude, spectral slope and midband fit were obtained from the spectroscopic analysis on the power spectra obtained from these measurements.

3. RESULTS AND DISCUSSION

3.1 Theoretical results

The average spectra of 250 signals from 250 random configurations of non-aggregated RBCs at 3 hematocrit levels are shown in figure 3(a). The results shown here are the non band-limited spectra obtained without taking into account a transducer with a finite receive bandwidth. It is clear from the figure that as the hematocrit of each sample increased, the spectral power generally increased over all frequencies. This increase in the power spectrum corresponds to a monotonic increase in the amplitude of the PA signals with increasing hematocrit. Since the PA signal amplitude is dependent on the concentration of the optical absorbers in the sample being irradiated, the increase in spectral power is due to the increase in the concentration of optical absorbers (the RBCs). The hematocrit is a direct measure of the concentration of RBCs. A similar trend in the amplitude of the PA signal amplitude with increasing hematocrit has been observed in other experimental studies[34]. It is important to note the dominant spectral frequency of the non-aggregated spectrum for each hematocrit level is related to the size of the optical absorber and does not change with concentration of absorbers[26]. We have previously shown experimentally that the PA spectral power of a single RBC predicted by the theoretical equations used in this simulation can be measured with high frequency ultrasound transducers (> 200 MHz) using a PA microscope with very high resolution[35].

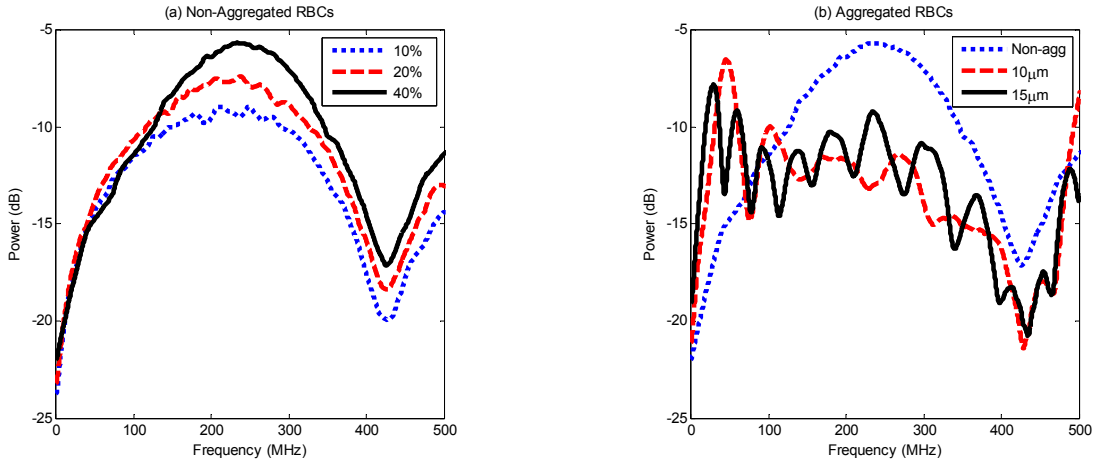

Figure 3. Average, non band-limited power spectra from (a) non-aggregated RBCs at 3 hematocrit levels and (b) aggregated RBCs at 3 aggregate sizes at 40% hematocrit. Not that in figure (b), the Non-agg spectrum corresponds to the non-aggregated spectrum at 40% hematocrit shown in figure (a).

The non band-limited simulated spectra from 250 random configurations of aggregated RBCs at 3 different aggregation levels at 40% hematocrit are shown in figure 3(b). The aggregates shown here with sizes of 10 and 15 μm were compared against the non-aggregated spectrum at 40% hematocrit shown in figure 3(a). It is observed for this figure that as the size of the aggregates increased, the dominant frequency of the power spectrum shifted towards lower frequencies

Downloaded from SPIE Digital Library on 19 Feb 2012 to 141.117.54.100. Terms of Use: http://spiedl.org/terms

(< 30 MHz). Enhancements in the spectral power of the 10 μm aggregate compared to the non-aggregated case were measured to be as high as 9 dB at 15 MHz. The shift of the spectral power towards lower frequencies in the presence of RBC aggregation has significant impact on the ability of PA spectroscopy to monitor changes that occur during the aggregation process. During the aggregation process, RBCs cluster closer to one another and their separation distance approaches the thermal diffusion length. It is the entire RBC aggregate size rather than individual RBCs' size that defines the dominant frequency of the PA signal. As a result, in a collection of aggregates, their spatial organization along with their size results in an increase in the signal strength at lower frequencies but a parallel decrease in the higher frequency signal strength (> 30 MHz). It should be noted that in a recent publication, Emelianov and colleagues reported on the theoretical and experimental environment-dependent generation of PA signals from plasmonic nanoparticles and suggested that the PA response is not from the nanosized absorber but rather from the interactions of the absorber with the low-absorbing surrounding medium[36]. This effect was not taken into account in these simulations but may be confined to signals from plasmonic nanoparticles.

The results shown in figure 3 suggest the potential of PA RF spectroscopy for the monitoring of the aggregation process. Significant changes were observed in the power spectra of aggregated RBCs of varying sizes compared to the non-aggregated case. This suggests that through PA spectroscopy, in principle, the changes that occur during RBC aggregation can be detected and monitored by observing the shifts that occur in the power spectra as the size of the aggregates increases. However, in practice, in order to be able to observe the significant frequency shifts occurring during RBC aggregation, one must use a very large (almost infinite) bandwidth transducer. Typical transducers used for PA experiments are either in the low frequency regime (< 15 MHz) for PA imaging[20] or (> 50 MHz) for PA microscopy[25]. All of these transducers have a finite, limited bandwidth. Since the size of the optical absorber will heavily control the spectral features of PA signals, the center frequency of the transducer and its bandwidth will significantly affect the detection process. In recent report, we utilized a Gaussian function for modeling a transducer with a finite bandwidth in order to take into account the effect of the transducer on the spectral features of the signal[31]. It was clear from this work that the transducer used played a significant role in the detection and monitoring of RBC aggregation.

PA spectroscopy can still be used for monitoring RBC aggregation even when band-limited signals obtained from a finite bandwidth, low frequency transducer are analyzed. Figure 4(a) shows the non band-limited spectra reported in figure 3(b) for a frequency up to 15 MHz. The spectra that are obtained by incorporating a 5 MHz transducer with a -6 dB 60% bandwidth are shown in figure 4(b). The transducer sensitivity profile greatly affects the shape and features of the PA RF spectra. At the central frequency of the transducer used, 5 MHz, there was a 3 and 5 dB increase in power for the 10 and 15 μm aggregate from the non-aggregated sample, respectively. Even for this frequency range, there are changes in the spectral slope of the PA RF signals, as shown in figure 4(c).

The normalized spectrum shown in figure 4(c) was obtained by subtracting the power spectra shown in figure 4(b) by the transducer response curve in a logarithmic scale. This yielded a linear curve over the -6 dB bandwidth of the transducer (2-8 MHz in this case) typically used as the most sensitive region of a transducer. Linear regression analysis was performed over the usable transducer bandwidth and the slope and midband fit (defined as the value of the linear fit evaluated at the midpoint of the usable transducer bandwidth) of each curve was extracted. The slope and midband fit for the non-aggregated RBCs as a function of hematocrit and aggregated RBCs as a function of aggregate size is shown in figure 4(d) and (e) respectively. For non-aggregated RBCs, the slope did not show statistically significant changes between each hematocrit level but there was a slight increase in the midband fit. The results obtained could be interpreted using what is already known from ultrasound tissue characterization (UTC) since both imaging modalities share similarities in the detected signals[27]. The spectral slope is primarily an indicator of scatterer (or absorber for PA RF analysis) shape and size. As the hematocrit increased, the shape and size of the RBCs did not change thus no significant changes in the slope of non-aggregated RBCs was observed. Furthermore, in UTC, the midband fit is a measure of US backscatter and it primarily depends on scatterer size and concentration. For the frequency range considered here, there was an increase in the midband fit with increasing hematocrit which suggests that the concentration of RBCs increased as the hematocrit increased.

Downloaded from SPIE Digital Library on 19 Feb 2012 to 141.117.54.100. Terms of Use: http://spiedl.org/terms

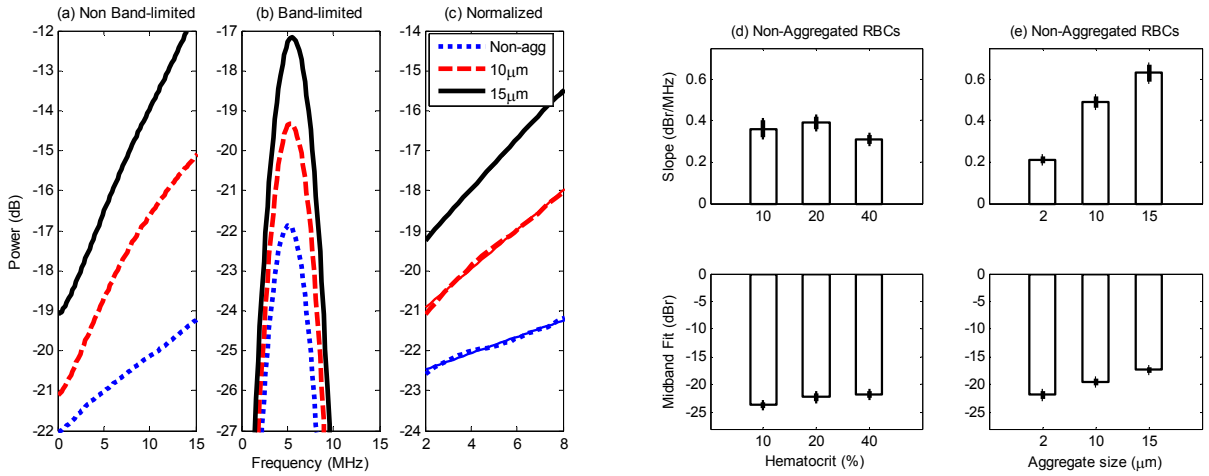

Figure 4. (a) Non band-limited power spectra from figure 3(b) for a frequency up to 15 MHz. (b) Band-limited power spectra obtained by filtering the spectra in (a) by the profile of a 5 MHz center frequency transducer (-6 dB 60% bandwidth). (c) Normalized power spectra obtained by subtracting the transducer sensitivity curve from the spectra in (b). The 2-8 MHz frequency range corresponds to the -6 dB transducer bandwidth. (d) Spectral slope and midband fit obtained for the normalized spectra of non-aggregated RBCs at 10, 20 and 40% hematocrit. (e) Spectral slope and midband fit obtained for the normalized spectra of aggregated RBCs with aggregate sizes of 2, 10 and 15 μm and 40% hematocrit.

Changes in the spectral parameters are more prominent as RBCs aggregate. The spectral parameters for aggregated RBCs are shown in figure 4(e). There is an increase in the spectral slope, doubling between the case for which there was no aggregation and when the aggregate size was 15 μm. This was due to the significant spectral shifts predicted by simulations (figure 3). The midband fit showed a significant increase as the size of the aggregates increased. This is in accordance with the relationship that exists between structural properties of the sample and the midband fit in UTC. In UTC, an increase in the scatterer size usually results in increased backscatter and thus increased midband fit; an increase in the size of the absorbers (the RBC aggregates) also results in increased photoacoustic signal at the frequencies of interest. It can be concluded from these observations that PA spectroscopy can monitor the changes that occur during RBC aggregation and can quantitatively assess the changes in the size and concentration of RBCs.

3.2 Experimental results

The experimental PA signal amplitudes, midband fit and spectral slopes at 3 hematocrit and 3 aggregation levels are shown in figure 5. As shown in figure 5(a), the amplitude of the PA signals monotonically increased with increasing hematocrit for non-aggregated RBCs. This was expected as well as predicted from the simulation results since the hematocrit is a direct measure of the concentration of the optical absorbers (the RBCs). Aggregation of RBCs was induced using various concentrations of Dextran-70 and suspending the non-aggregated RBCs in the Dextran-PBS solutions for each hematocrit level used. A non-linear behaviour of the PA signal is observed with increasing Dextran-PBS concentration. For all the hematocrit levels, a Dextran-PBS concentration of 3% gave the highest PA signal amplitude while 1 and 8% solutions had similar amplitudes. All the amplitudes of the aggregated solutions, at all hematocrit levels, were higher than the non-aggregated case (0% [Dextran-PBS]). The non-linear trend in PA signal amplitude as a function of Dextran concentration has been reported using independent techniques of optical techniques discussed in the introduction[37]. These results suggest that PA imaging has the potential to monitor the aggregation of RBCs for at various hematocrit levels.

Downloaded from SPIE Digital Library on 19 Feb 2012 to 141.117.54.100. Terms of Use: http://spiedl.org/terms

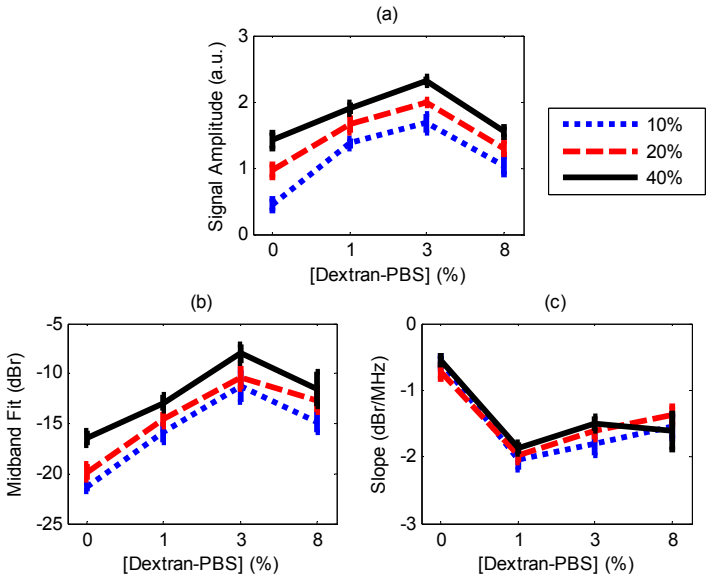

Figure 5. (a) PA signal amplitude, (b) midband fit and (c) spectral slope for porcine RBCs at 3 hematocrit levels and 3 aggregation levels. Note that a 0% [Dextran-PBS] concentration refers to the non-aggregated RBC samples at each hematocrit.

The midband fit and slope of the experimental results are shown in figure 5(b) and (c), respectively. Similar to the PA signal amplitude curve (figure 5(a)), the midband fit shows the same behaviour with increasing Dextran-PBS concentration. For a concentration of 0% [Dextran-PBS], the midband fit increases with increasing hematocrit. The highest value of the midband fit was observed to occur for a Dextran-PBS concentration of 3% where the highest degree of aggregates occurred. Enhancements similar to those reported for the simulated results were observed for the highest degree of aggregation compared to non-aggregated RBCs. The spectral slope, a measure of the scatterer size, decreased as the samples formed aggregates. During aggregation, the RBCs cluster closer together and form larger absorbing structures than non-aggregating RBCs. In both the theoretical and experimental results, an increase of the spectral slope of a factor of 2 is predicted / measured. However, whereas the theory predicts positive spectral slopes (figure 4(c)), in the experiments a negative slope is measured (figure 5(c)). This discrepancy may be due to the normalization procedure used (the gold film) and is currently being examined. Moreover, there are no observable changes in the slope as a function of hematocrit. This is due to the fact that in using a 5 MHz center frequency transducer there are no observable shifts in the dominant frequency of the signals as observed from the band-limited spectra in figure 4(d).

The results obtained here strongly suggest the potential of PA spectroscopy for monitoring the changes that occur during RBC aggregation. Aggregation is a phenomenon that results in significant changes in the size and shape of the RBC morphology. PA spectroscopy seems to be sensitive enough to be able to detect changes in the size and concentration of absorbers. The shifts in the dominant frequency of the PA signal due to the increase of aggregate size seem to be a robust variable for monitoring changes during RBC aggregation. In addition, by taking into account the sensitivity of the transducer used for the measurements, one can use spectral parameters such as the slope and the midband fit of the normalized spectra in order to characterize the RBC samples. The relationship between these parameters and tissue properties during PA measurements is yet to be determined but the theoretical results presented in this paper provide some insight into this relationship. The advantage of PA over US for monitoring RBC aggregation phenomena lies in the fact that PA has a simpler relationship between the signal amplitude and hematocrit. While in US it is difficult to judge the hematocrit level from the backscattered power, in PA the linear relationship between signal amplitude and hematocrit makes is simpler to infer the hematocrit level from the signal amplitude. In addition, the ability of PA to probe the oxygen depended absorption of blood provides the strong advantage of obtaining functional information in addition to the structural information provided by the PA RF spectroscopy. It is possible in principle to monitor the oxygenation changes during the aggregation process by using multiple wavelengths to probe the various absorption peaks of blood at different oxygenation levels. The techniques established here could potentially provide a non-invasive approach towards

Downloaded from SPIE Digital Library on 19 Feb 2012 to 141.117.54.100. Terms of Use: http://spiedl.org/terms

detecting the oxygenation level of blood prior and during the aggregation of RBCs and use that information as an indicator for making important clinical decisions.

4. CONCLUSIONS

This paper discusses the potential of using PA spectroscopy for monitoring changes that occur during the aggregation of RBCs. A theoretical model was presented to demonstrate how RBC aggregation could be detected by examining the spectral features of the PA signals. Using spectroscopic techniques adopted from ultrasound tissue characterization methods, we have shown the ability of PA to monitor and characterize the phenomenon of RBC aggregation. This study suggests that PA has the potential of being used as a non-invasive tool for assessing RBC aggregation.

ACKNOWLEDGEMENTS

The support of the following funding agencies is gratefully acknowledged: NSERC, CIHR, CFI and the Canada Research Chairs program awarded to M. C. Kolios. E. Hysi is supported through the NSERC Alexander Graham Bell Canada Graduate Scholarship program. The authors acknowledge Jennifer Barry (Comparative Research, Sunnybrook Research Institute) and Arthur Worthington (Ryerson University) for their technical assistance during this work.

REFERENCES

[1] Cardoso, A. V., Pereira, H., Marcondes, G. D., Ferreira, A. D. and Araujo, P. R., "Microplate reader analysis of triatomine saliva effect on erythrocyte aggregation," Mater. Res. 10(1), 31-36 (2007).
[2] Meiselman, H. J., "Red blood cell aggregation: 45 years being curious," Biorheology 46, 1-9 (2009).
[3] Brooks, D. E., [Mechanism of Red Blood Cell Aggregation in Blood Cells, Rheology and Aging], Springer Verlag,Berlin, 158-162 (1988).
[4] Baumler, H., Neu, B., Mitlohner, R., Georgieva, R., Meiselman, H. J. and Keisewetter, H., "Electrophoretic and aggregation behavior of bovine, horse and human red blood cells in plasma and in polymer solutions," Biorheology 38, 39-51 (2001).
[5] Baskurt, O.K., Neu, B. and Meiselman, H.J., [Red Blood Cell Aggregation], CRC Press, Boca Raton, 1-35, (2011).
[6] Baskurt, O.K., Hardeman, M. R., Rampling, M. W. and Meiselman, H. J., [Handbook of Hemorheology and Hemodynamics], IOS Press, Amsterdam, 45-49, (2007).
[7] Baskurt, O. K., Temiz, A. and Meiselman, H. J., "Red blood cell aggregation in experimental sepsis," J. Lab. Clin. Med. 130(2), 183-190 (1997).
[8] Almog, B., Gamzu, R., Amlog, R., Lessing, J. B., Shapira, I., Berliner, S., Pauzner, D., Maslovitz, S. and Levin, I., "Enhanced erythrocyte aggregation in clinically diagnosed pelvic inflammatory disease," Sex. Transm. Dis. 32,484-486 (2005).
[9] Foresto, P., D'Arrigo, M., Filippin, F., Gallo, R., Barberena, L., Racca, L., Valdere, J. and Rasia, R. J., "Hemorheological alterations in hypertensive patients," Medicine-Buenos Aire. 65, 121-125 (2005).
[10] Chong-Martinez, B., Buchanan, T. A., Wenby, R. B. and Meiselman, H. J., "Decreased red blood cell aggregation subsequent to improved glycaemic control in type 2 diabetes mellitus," Diabetic Med. 20, 301-306 (2003).
[11] Plebani, M. and Piva, E., "Erythrocyte sedimentation rate: Use of fresh blood for quality control," Am. J. Clin. Pathol. 117, 621-626 (2002).
[12] Baskurt, O. K., Yalcin, O., Ozdem, S., Armstrong, J. K. and Meiselman, H. J., "Hemorheological parameters as determinants of myocardial tissue hematocrit values," Clin. Hemorheol. Micro. 35, 45-50 (2006).
[13] Dobbe, J. G. G., Streekstra, G. J., Strackee, J., Rutten, M. C. M., Stijnen, J. M. A. and Grimbergen, C. A.,"Syllectometry: The effect of aggregometer geometry in the assesment of red blood cell shape recovery and aggregation," IEEE T. Bio-Med. Eng. 50, 97-106 (2003).
[14] Shung, K. K. and Thieme, G. A., [Biological Tissue as Ultrasonic Scattering Media in Ultrasonic Scattering in Biological Tissue], CRC Press, Boca Raton, 57-59 (1993).
[15] Yu, F. T. H., Armstrong, J. K., Tripette, J., Meiselman, H. J. and Cloutier, G., "A local increase in red blood cell aggregation can trigger deep vein thrombosis: evidence based on quantitative cellular ultrasound imaging," J.Thromb. Haemost. 9, 481-488 (2011)
[16] Cobbold, R. S. C., [Foundations of Biomedical Ultrasound], Oxford University Press, New York, 100-123, (2007).
[17] Wang, L. V., "Prospects of photoacoustic tomography," Med. Phys. 35(12), 5758-2767 (2008).
[18] Wang, L. V., [Photoacoustic Imaging and Spectroscopy], CRC Press, Boca Raton, 20-57, (2009).

Downloaded from SPIE Digital Library on 19 Feb 2012 to 141.117.54.100. Terms of Use: http://spiedl.org/terms

[19] Ntziachristos, V., Ripoll, J., Wang, L. V. and Weissleder, R., "Looking and listening to light: the evolution of whole-body photonic imaging," Nat. Biotechnol. 23(3), 313-320 (2005).
[20] Wang, X., Xie, X., Ku, G., Wang, L. V. and Stoica, G., "Noninvasive imaging of hemoglobin concentration and oxygenation in rat brain using high-resolution photoacoustic tomography," J. Biomed. Opt. 11(2), 024015-1-(2006).
[21] Emelianov, S. Y., Li, P. and O'Donnell, M., "Photoacoustics for molecular imaging and therapy," Phys. Today 62(5), 34-39 (2009).
[22] Zalev, J. and Kolios, M. C., "Detecting abnormal vasculature from photoacoustic signals using wavelet-packet features," Proc. SPIE 7899, 78992M-1-15 (2011).
[23] Patterson, M. P., Riley, C. P., Kolios, M. C. and Whelan, W. M., "Optoacoustic signal amplitude and frequency spectrum analysis laser heated bovine liver ex-vivo," Proc. IEEE IUS, in press (2011).
[24] Soroushian, B., Whelan, W. M. and Kolios, M. C., "Study of laser-induced thermoelastic deformation of native and coagulated ex-vivo bovine liver tissue for estimating their optical and thermomechanical properties," J. Biomed. Opt. 15(6), 065002-1-10 (2010).
[25] Strohm, E., Rui, M., Gorelikov, I., Matsuura, N. and Kolios, M. C., "Vaporization of perfluorocarbon droplets using optical irradiation," Biomed. Opt. Express 2(6), 1432-1442 (2011).
[26] Diebold G. J., [Photoacoustic Monopole Radiation: Waves from Objects with Symetry in One, Two and Three Dimensions in Photoacoustic Imaging and Spectroscopy], CRC Press, Boca Raton, 3-17 (2009).
[27] Lizzi, F. L., Ostromogilsky, M., Feleppa, E. J., Rorke, M. C. and Yaremko, M. M., "Relationship of ultrasonic parameters to features of tissue microstructure," IEEE T. Ultrason. Ferr. 33(3), 319-329 (1987).
[28] Kolios, M. C. and Czarnota, G. J., "Potential use of ultrasound for the detection of cell changes in cancer treatment," Future Oncol. 5(10), 1527-1532 (2009).
[29] Saha, R. K. and Kolios, M. C., "A simulation study on photoacoustic signals from red blood cells," J. Acoust. Soc. Am. 129(5), 2395-2943 (2011).
[30] Saha, R. K. and Kolios, M. C., "Effects of erythrocyte oxygenation on optoacoustic signals," J. Biomed. Opt.16(11), 115003-1-9 (2011).
[31] Hysi, E., Saha, R. K., Rui, M. and Kolios, M. C., "Detection and characterization of red blood cell (RBC) aggregation with photoacoustics," Proc. SPIE, in press (2012).
[32] Saha, R. K., Hysi, E. and Kolios, M. C., "A simulation study on the photoacoustic signals from non-aggregating and aggregating erythrocytes," Ultrasonic Imaging, 33(4), 29-30 (2011).
[33] Hysi, E., Saha, R. K. and Kolios, M. C., "Characterization of red blood cell aggregation with photoacoustics: A theoretical and experimental study," Proc. IEEE IUS, in press (2011).
[34] Karpiouk, A. B., Aglyamov, S. R., Mallidi, S., Shah, J., Scott, W. G., Rubin, J. M. and Emelianov, S. Y., "Combined ultrasound and photoacoustic imaging to detect and stage deep vein thrombosis: phantom and ex vivo studies," J. Biomed. Opt. 13(5), 054061-1-1-8 (2008).
[35] Rui, M., Bost, W., Weiss, E. C., Lemor, R. and Kolios, M. C., "Photoacoustic microscopy and spectroscopy of individual red blood cells," OSA Opt. & Photo. Congress BIOMED/DH, BSuD93 (2010).
[36] Chen, Y., Frey, W., Aglyamov, S. and Emelianov, S., "Environment-dependent generation of photoacoustic waves from plasmonic nanoparticles," Small 8(1), 47-52 (2012).
[37] Baskurt, O. K., Farley, R. A. and Meiselman, H. J., "Erythrocyte aggregation tendency and cellular properties in horse, human and rat: a comparative study," Am. J. Physiol. Heart Circ. Physiol. 273, H2604-H2612 (1997).

Downloaded from SPIE Digital Library on 19 Feb 2012 to 141.117.54.100. Terms of Use: http://spiedl.org/terms